Hemojuvelin N-terminal mutants reach the plasma membrane but do not activate the hepcidin response

Alessia Pagani, Laura Silvestri, Antonella Nai, and Clara Camaschella

Vita Salute University IRCCS San Raffaele, Milan, Italy

ABSTRACT

Background
Hemojuvelin is a glycosylphosphatidylinositol-anchored protein, expressed in liver, skeletal muscle and heart. As a co-receptor of bone morphogenetic protein, membrane hemojuvelin positively modulates the iron regulator hepcidin. Mutations of the gene encoding for hemojuvelin cause juvenile hemochromatosis, characterized by hepcidin deficiency and severe iron overload. We have previously shown that several hemojuvelin variants do not efficiently reach the plasma membrane, whereas a few N-terminal mutants localize to the plasma membrane.

Design and Methods
We studied hemojuvelin mutants of N-terminus (C80R, S85P, G99V, ΔRGD) and GDPH-consensus site for autoproteolysis (A168D, F170S, D172E) transiently expressed in HeLa cells, using electron microscopy, morphometric analysis and binding assays at different time points. Hepcidin activation by wild-type and mutant forms of hemojuvelin was assessed in Hep3B cells transfected with a hepcidin-promoter luciferase-reporter construct.

Results
S85P, G99V and ΔRGD were localized to plasma membrane 36 hours after transfection, but less efficiently exported than the wild-type protein at earlier (24-30 hours) times. Morphometric analysis clearly documented delayed export and endoplasmic reticulum retention of G99V. C80R was exported without delay. GDPH variants were partially retained in the endoplasmic reticulum and Golgi apparatus, but showed impaired plasma membrane localization. In the hepcidin promoter assay only wild type hemojuvelin was able to activate hepcidin.

Conclusions
The delayed export and retention in the endoplasmic reticulum of some N-terminal mutants could contribute to the pathogenesis of juvenile hemochromatosis, reducing a prompt response of bone morphogenetic protein. However, independently of their plasma membrane export, all hemojuvelin mutants tested showed no or minimal hepcidin activation.

Key words: juvenile hemochromatosis, hemojuvelin, hepcidin, protein-processing and trafficking.

Citation: Pagani A, Silvestri L, Nai A, and Camaschella C. Hemojuvelin N-terminal mutants reach the plasma membrane but do not activate the hepcidin response. Haematologica 2008; 93:1466-1472. doi: 10.3324/haematol.12508

Acknowledgments: we acknowledge Paolo Arosio for the gift of anti-HJV antibody and Sonia Levi for discussion. We thank Roman Polishchuk from the Telethon Electron Microscopy Core Facility (TeEMCoF; Consorzio Mario Negri Sud - Santa Maria Imbaro) for the immuno electron microscopy and morphometric analyses.

Funding: this work was supported by Telethon Rome grant GGP05024, and EEC Framework 6 (LSHM-CT-2006-037296 EuroIron1) and Progetto di Rilevante Interesse Nazionale (PRIN), Ministero dell'Università e della Ricerca funds to CC.

Manuscript received November 13, 2007. Revised version arrived May 14, 2008. Manuscript accepted June 23, 2008.

Correspondence:
Clara Camaschella,
Università Vita-Salute San Raffaele,
via Olgettina 60,
20132 Milano, Italy.
E-mail: camaschella.clara@hsr.it

Introduction

Hemojuvelin (HJV) is a glycosylphosphatidylinositol (GPI)-anchored protein that belongs to the repulsive guidance molecule (RGM) family. While its homologous proteins RGMa and RGMb are expressed in the central nervous system and involved in axon guidance and neural tube closure, HJV (or RGMc) is expressed in the same tissues as the iron regulatory peptide hepcidin, such as the liver and heart, and in skeletal muscle, and has an important role in hepcidin regulation.

Different mutations of *HJV* are responsible for juvenile hemochromatosis (or type 2 hemochromatosis),[1] a severe disease with an early onset, characterized by hepcidin insufficiency which leads to clinical complications of iron overload, in particular hypogonadism and cardiomyopathy. Patients with juvenile hemochromatosis caused by *HJV* mutations (type 2A) share the same phenotype as that of patients with mutations that disrupt the hepcidin gene (*HAMP*, type 2B).[2] The central role of HJV in body iron homeostasis is supported by the evidence that *Hjv* knockout mice (*Hjv*$^{-/-}$ mice) show severe suppression of hepatic hepcidin and increased iron deposition in the liver, pancreas and heart.[3,4]

HJV encodes a protein characterized by a N-terminal signal peptide, a RGD integrin binding motif, a partial von Willebrand factor type D domain containing a glucose-6-phosphate dehydrogenase (GDPH) consensus sequence for autoproteolysis, a RNRR consensus sequence for furin cleavage[5,6] and a C-terminal GPI-anchor domain.

HJV is localized to the plasma membrane, through the GPI-motif, as cleaved N- (16 kDa) and C-terminal (30 kDa) fragments linked together by disulphide bonds.[7] Membrane-HJV (m-HJV) is a co-receptor for bone morphogenetic protein (BMP), which participates in the activation of hepcidin transcription.[8,9]

HJV also exists as a soluble protein (s-HJV) produced by furin cleavage and secreted into the extracellular environment. s-HJV acts as an antagonist in the hepcidin activation pathway, sequestering BMP and interrupting their signaling.[10] Large amounts of s-HJV are released into cellular media in conditions of iron deficiency[6] and this soluble protein is reduced in conditions of iron overload.[11] s-HJV is present in two forms, a major one of 42 kDa and a minor one of 30 kDa.

In a previous study we demonstrated that defective autoproteolytic processing hampers the correct targeting of several mutants to the plasma membrane and causes their retention in the endoplasmic reticulum. Based on these findings we suggested that the lack of plasma membrane presentation is a pathogenetic mechanism of juvenile hemochromatosis, at least for mutants affecting the C-terminal part of the protein.[11] In this study we investigated the export of N-terminal HJV variants to the cell surface and their effect on hepcidin activation.

Design and Methods

Generation of wild-type and hemojuvelin mutants

The whole *HJV* open reading frame was amplified from human cDNA and cloned into the mammalian vector pcDNA3.1(+) (Invitrogen, Carlsbad, CA, USA) to obtain the pcDNA3.1-*HJV* construct. For some experiments a cMYC tag was introduced at the end of the signal peptide, at position 37, to produce the pcDNA3.1-*HJV*$^{37\text{-}MYC}$ construct.[11]

Mutant constructs. HJV cDNA was mutagenized using pcDNA3.1-*HJV*$^{37\text{-}MYC}$ or pcDNA3.1-*HJV* as a template and the QuickChange site-directed mutagenesis kit (Stratagene, La Jolla, CA, USA), according to the manufacturer's protocol. The oligonucleotides used are listed in Table 1 and in the paper by Silvestri *et al*.[11]

Cell culture

Cell culture media and reagents were obtained from Invitrogen and Sigma-Aldrich (St. Louis, MO, USA).

HeLa cells, which do not express endogenous HJV, and Hep3B cells were cultured, respectively, in Dulbecco's modified Eagle's medium (DMEM) and in Earl's minimal essential medium (EMEM), supplemented with 2 mM L-glutamine, 200 U/mL penicillin, 200 mg/mL streptomycin, 1 mM sodium pyruvate, and 10% heat-inactivated fetal bovine serum (FBS) at 37°C in 95% humidified air and 5% CO_2.

Western blot analysis

HeLa cells, seeded in 100-mm-diameter dishes up to 70-80% of confluency, were transiently transfected with 20 μg of plasmid DNA and 50 μL of the liposomal transfection reagent Lipofectamine 2000 (Invitrogen) in 3 mL of OptiMem (Invitrogen) according to the manufacturer's instructions. After 18 hours the medium was replaced with 4 mL of OptiMem and 24 hours later media were collected and concentrated using Amicon Ultra (Millipore Corporation, Billerica, MA, USA). The cells were lysed in RIPA buffer. Proteins were quantified using the Bio-Rad Protein Assay (Bio-Rad, Hercules, CA, USA): equal amounts of total proteins (50 μg) were subjected to 10% sodium dodecyl sulfate polyacrylamide gel electrophoresis (SDS-PAGE), and then transferred to

Table 1. Primers used for *HJV* mutagenesis.

Amino acid substitution	*Sense*	*Antisense*
C80R	5'-tctggcggcctcCGTcgagccctccgc-3'	5'-gcggagggctcgACGgaggccgccaga-3'
S85P	5'-cgagccctccgcCCCtatgcgctctgc-3'	5'-gcagagcgcataGGGgcggagggctcg-3'
A168D	5'-cggggttcttgcattgcGATtccttcggggaccccccatg-3'	5'-catgggggtccccgaaggaATCgcaatgcaagaaccccg-3'
D172E	5'-cattgcgcttccttcgggGAAccccatgtgcgcagcttc-3'	5'-gaagctgcgcacatggggTTCcccgaaggaagcgcaatg-3'
ΔRGD	5'-gcaccgcccgcacctgcctcgccttccattcggc-3'	5'-gccgaatggaaggcgaggcaggtgcgggcggtgc-3'

Hybond C membrane (Amersham Biosciences Europe GmbH, Freiburg, Germany) using a standard western blotting technique. Blots were blocked with 2% ECL Advance Blocking Agent (Amersham Biosciences) in TBS (0.5 M Tris-HGI pH 7.4 and 0.15 M NaCl) containing 0.1% Tween-20 (TBST), and incubated for 2 hours with rabbit-anti-HJV (1:1000).[6] After washing with TBST, blots were incubated for 1 hour with relevant horse radish peroxidase-conjugated secondary antisera (goat-anti-rabbit-horse radish peroxidase antibody, 1:100000) and developed using a chemiluminescence detection kit (ECL, Amersham Biosciences). The intensity of bands was quantified using ImageJ software.

Cell surface hemojuvelin expression: quantification by binding assays

Cell surface expression of HJV was quantified as described by Silvestri *et al.*[11] In brief, 10^4 HeLa cells were seeded in 48-well plates and transfected with 0.4 μg of plasmid DNA using 1 μL of Lipofectamine 2000. After 20, 24, 30 and 36 hours cells, fixed with 4% paraformaldehyde, were washed with phosphate-buffered saline, blocked with 5% non-fat milk in phosphate-buffered saline, incubated 2 hours with rabbit-anti-HJV (1:1000)[6] and then with the relevant secondary horse radish peroxidase antibody (goat-anti-rabbit-horse radish peroxidase antibody, 1:1000), at 37°C for 1 hour. In order to determine total HJV expression, cells were permeabilized with 0.1% Triton X-100 in phosphate-buffered saline, with prior blocking and incubation with anti-HJV. Peroxidase activity was measured with an HSR substrate (o-phenylenediamine dihydrochloride, OPD; Sigma), according to the manufacturer's instructions. The amount of m-HJV was calculated as a ratio between the absorbance of unpermeabilized and permeabilized cells, as already described.[11,12] Background absorbance was subtracted for each sample. Student's t-test was used for statistical calculations.

Immuno-electron microscopy analyses

HeLa cells were transiently transfected using Lipofectamine 2000 with wild-type (WT), G99V and D172E HJV expressing vectors, as described previously.[13] Cells were fixed with a mixture of 4% paraformaldehyde and 0.05% glutaraldehyde at different time points (6, 12 and 18 hours), labeled with goat polyclonal anti-cMYC (Novus Biological, Littelton, CO, USA) using the gold-enhance protocol, embedded in Epon-812, and cut as described previously.[11,14] Electron microscope images were acquired from thin sections under a Philips Tecnai-12 electron microscope (Philips, Einhoven, the Netherlands) using an ULTRA VIEW CCD digital camera. Thin sections were also used for the quantification of gold particles residing within different intracellular compartments.

Hepcidin promoter luciferase reporter construct

A pGL2-basic reporter vector (Promega, Madison, WI, USA) containing a 2.9 Kb fragment of the human hepcidin promoter (Hep-Luc) has been developed. This fragment encompasses the BMP responsive regions between –260 bp and +1, both in human and murine promoters and includes the human sequences from –2450 bp to –2200 bp. This latter region corresponds to sequences –1800 bp and –1600 bp in the murine *Hamp1* promoter,[15] based on the alignment of *Hamp1* and human hepcidin promoter sequences using the Genomatix DiAlign TF software (Genomatix Software GMBH 1998-2008).

Luciferase assay

Hep3B cells, seeded at 70-80% confluency, were transiently transfected with 0.25 μg hepcidin promoter luciferase reporter construct in combination with pRL-TK Renilla luciferase vector (Promega) to control transfection efficiency, and with 0.1 μg/mL of cDNA encoding wild type or mutant HJV. Eighteen hours after transfection the medium was changed, cells were starved of serum for 24 hours in EMEM supplemented with 2% fetal bovine serum, and then lysed. Luciferase activity was determined according to instructions of the manufacturer of the assay kit (Promega Dual Luciferase Reporter Assay). Experiments were performed in triplicate. Relative luciferase activity was calculated as the ratio of firefly (reporter) to Renilla (transfection control) luciferase activity and is expressed as a multiple of the activity of cells transfected with the reporter alone.

Results

Processing and membrane presentation of the mutants studied

The HJV variants studied are shown in Figure 1A. C80R[16] and S85P localize at the N-terminus of the protein, A168D is in the proximity of and D172E disrupts the GDPH consensus sequence.[17] We also generated an artificial protein from which the entire RGD domain was deleted (ΔRGD). All the variants were transiently expressed in HeLa cells and analyzed for processing, plasma membrane export and ability to release a soluble protein. As shown by the presence of the 30 kDa fragments (Figure 1B, upper panel), C80R, S85P and ΔRGD variants undergo autoproteolysis, as do WT and G99V HJV.[11] A168D and D172E are not cleaved, as previously shown for F170S.[11]

All the mutants released soluble forms into culture media (Figure 1B, lower panel), with different ratios between the 42 kDa and the 30 kDa species (histogram in Figure 1B). The 42 kDa species was the prevalent form for the WT, S85P, G99V, and ΔRGD proteins, it was the only form detectable for the cleavage-defective variants and was a minor component in C80R.

In order to quantify the amounts of WT and mutant proteins localized on HeLa cells we used a surface labeling method. Thirty-six hours after transfection all N-terminal mutants reached the plasma membrane with the same efficiency as that of the WT protein. The complete deletion of amino acids 98-100 of the RGD domain did not cause a more severe defect than the single amino acid substitution of G99V. In contrast the export of GDPH variants to the cell surface was significantly reduced (Figure 1C).

The plasma membrane export of most N-terminal mutants is delayed

Since the N-terminal variants are cleaved and reach the plasma membrane, the pathogenetic mechanism for these mutants remained unclear. We previously noted that G99V, although efficiently reaching the plasma membrane 36 hours post-transfection, is partially retained in the endoplasmic reticulum, suggesting a delay in its processing to the cell surface. Electron microscopy studies (Figure 2A) and morphometric analyses (Figure 2B) performed 6, 12 and 18 hours after transfection confirmed the delayed intracellular trafficking and cell surface presentation of G99V. To examine whether this delay is common to other N-terminal variants (C80R, S85P, G99V, C119F and ΔRGD), we set up a simplified time course analysis using a binding assay. Analyses were carried out at different times points since this assay is less sensitive than electon microscopy and morphometric analysis and requires different transfection conditions. We confirmed a delay in plasma membrane export 24 hours and 30 hours after transfection for all N-terminal variants, the only exception being C80R, which behaves as the WT protein (Figure 2C).

Plasma membrane localization of GDPH-defective mutants is impaired

We studied the intracellular trafficking of D172E as representative of GDPH-defective variants by electron microscopy (*data not shown*) and morphometric analyses (Figure 3). As previously demonstrated for F170S, 18 hours after transfection D172E, although partially retained in the endoplasmic reticulum, was present in the Golgi apparatus but showed impaired plasma membrane localization.

WT but not mutant hemojuvelin stimulates hepcidin promoter activity

WT HJV and some representative N-terminal (C80R, G99V and ΔRGD), GDPH-defective (D172E) and C-terminal (G320V) variants were analyzed for their ability to activate the hepcidin promoter. The activation of hepcidin promoter was analyzed in Hep3B cells, transiently transfected with WT or mutant HJV and the hepcidin promoter luciferase reporter construct. WT HJV had a strong activating effect (about 8 fold as compared to a control), while N-terminal, cleavage and C-terminal variants had minimal or no effect (Figure 4).

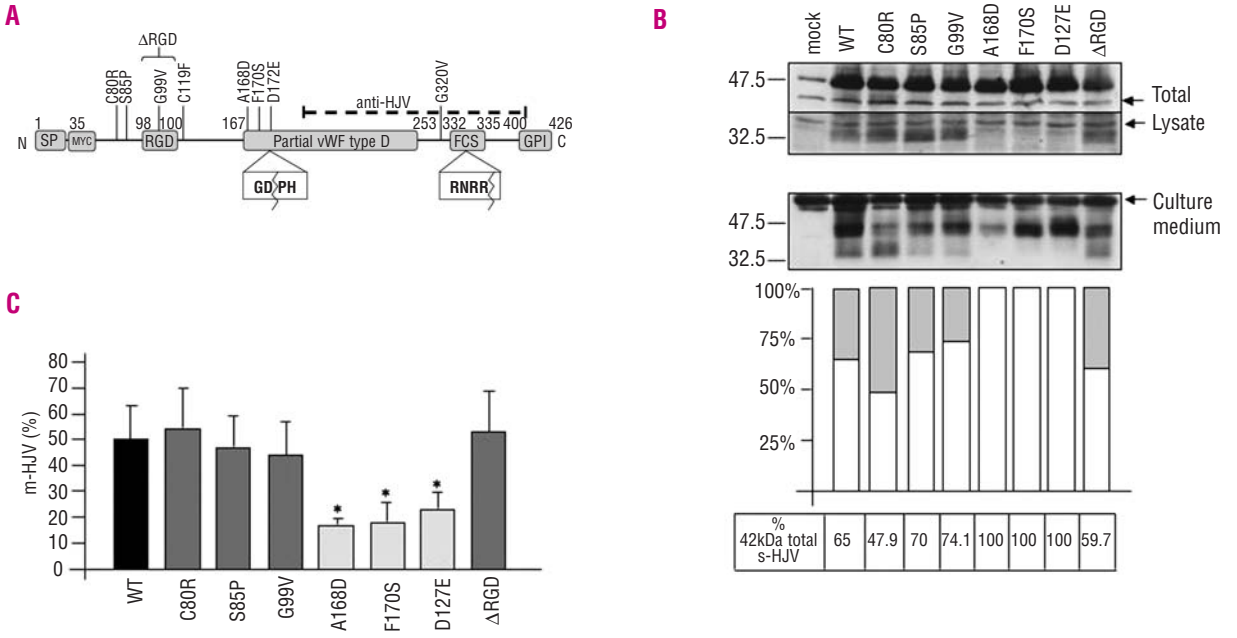

Figure 1. Characterization of the HJV variants studied. (A) Schematic representation of HJV functional domains and of the mutants studied. SP indicates signal peptide; RGD: arginine-glycine-aspartic acid integrin-binding domain. The cMYC tag, GDPH autoproteolytic site, and furin cleavage site (FCS) are indicated. Numbers refers to amino acids. The dotted line shows the peptide recognized by the anti-HJV antibody. Missense mutations and the artificial ΔRGD variant are shown. (B) Processing and secretion of WT and mutant HJV. HeLa cells were transiently transfected with the empty vector (mock), WT, C80R, S85P, G99V, A168D, F170S, D172E and ΔRGD constructs. After 36 hours, cell culture media were concentrated and cells were collected and lysed in RIPA buffer. Fifty micrograms of proteins were separated on 10% SDS-PAGE and analyzed by western blot using the anti-HJV antibody. Scales refer to relative molecular mass in kilodaltons (kDa). Arrows indicate non-specific bands. A further non-specific band is recognized by the anti-HJV antibody at about 47.5 kDa, as shown in the mock lane. The histogram illustrates the results of the densitometric analysis of s-HJV species expressed as percentages (%) of total s-HJV. The intensity of the bands was determined using ImageJ software. White bars: 42 kDa s-HJV; gray bars: 30 kDa s-HJV. The experiments were performed in triplicate and a representative experiment is shown. (C) Plasma membrane localization of WT protein and HJV mutants. Transfected HeLa cells were fixed and incubated with anti-HJV for the binding assays. The amount of HJV expressed at the cell surface (non-permeabilized cells) is shown as a fraction (%) of total protein expression (permeabilized cells). Black bars: WT HJV; dark gray bars: N-terminal variants; gray bars: GDPH-defective variants. Statistical significance was calculated on three independent experiments, conducted in triplicate. *$p<0.005$.

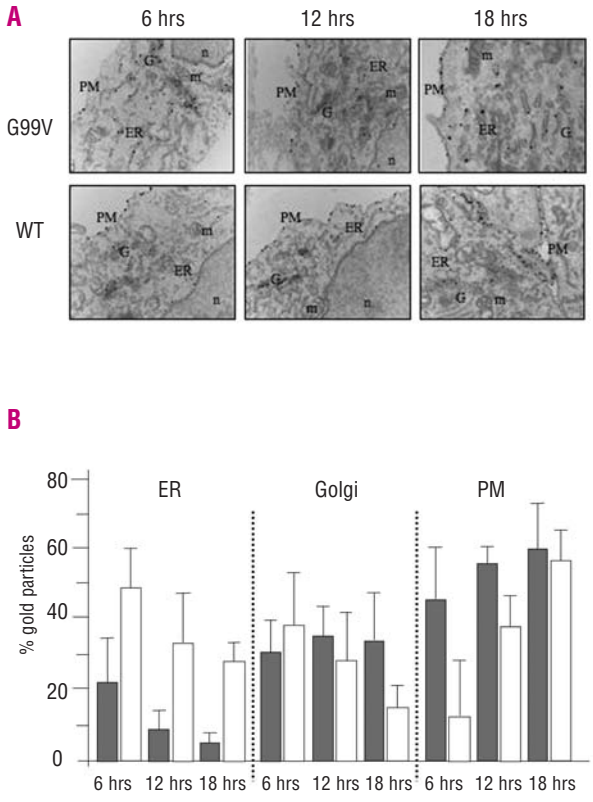

Figure 2. Time course analyses of the distribution of N-terminal mutants. Electron microscopy (A) and morphometric analysis (B) of wild-type (WT) and G99V hemojuvelin were used to follow the distribution of the molecules in intracellular compartments at different time points. HeLa cells were transiently transfected with WT and G99V HJV constructs. At 6, 12 and 18 hours after transfection, sections were stained with antibody against cMYC using a nano-gold protocol (see the *Design and Methods* section for details). Images were acquired using AnalySIS software (Soft Imaging System, Lakewood, CO, USA). Original magnification, × 23000. PM: plasma membrane; ER: endoplasmic reticulum; G= Golgi; m: mitochondria; n: nucleus. Gray bars: WT HJV; white bars: G99V. Error bars indicate standard deviations (SD). (C) Time course analysis using binding assays. HeLa cells were transiently transfected with mammalian vectors encoding WT HJV, C80R, S85P, G99V, C119F mutants and DRGD. m-HJV was quantified at 20, 24, and 30 hours post-transfection. The quantity of HJV expressed at the cell surface (non-permeabilized cells) is shown as a fraction (%) of total protein expression (permeabilized cells). The statistical significance of the differences between mutants and WT was calculated from a representative experiment, conducted in triplicate. *p<0.01; **p<0.005.

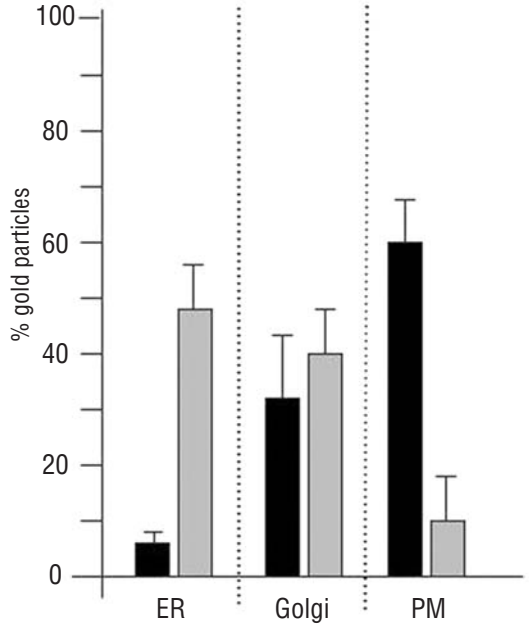

Figure 3. Intracellular trafficking of GDPH-defective mutants. Morphometric analysis of wild-type (WT) and D172E HJV was used to follow the distribution of the molecules in intracellular compartments 18 hours post-transfection, as described in the legend to Figure 2B. Black bars: WT HJV; gray bars: D172E. Error bars indicate standard deviations (SD).

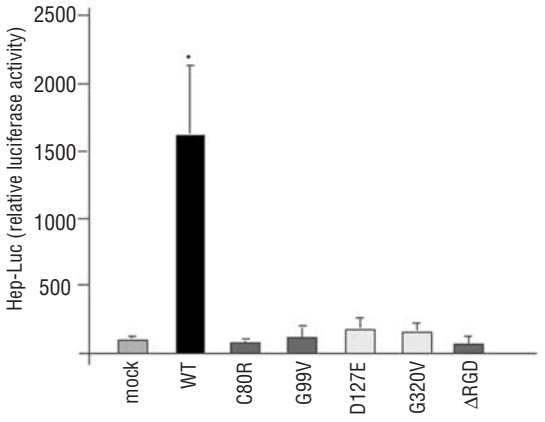

Figure 4. Effect of wild-type (WT) and mutant hemojuvelin on hepcidin activation. Hep3B cells were transfected with the hepcidin promoter firefly luciferase reporter (Hep-Luc), pRL-TK Renilla luciferase vector (used for transfection efficiency normalization) and with empty vector (mock), WT and mutants (C80R, G99V, DRGD, D172E, G320V) HJV. About 42 hours later cell lysates were analyzed for luciferase activity. The experiments were performed three times in triplicate and the values shown, expressed as relative luciferase activity, refer to a representative assay. White bar: mock; black bar: WT HJV; dark gray bars: N-terminal variants (C80R, G99V, DRGD); gray bars: C-terminal variants (D172E, G320V). Error bars indicate standard deviations. The statistical significance of the differences between mock and hemojuvelin was calculated from a representative experiment, conducted in triplicate. *p<0.005.

Discussion

The results of this study confirm and extend previous observations on HJV pathogenetic mutants. We previously determined that the inability of several mutants to be targeted to plasma membrane in the appropriate cleaved form[11] is a common pathogenetic mechanism of juvenile hemochromatosis. However, during that research we observed that the ability of G99V and C119F mutants to reach the plasma membrane was not or only partially affected, respectively. In this study we investigated the processing and export of G99V and other N-terminal mutants in more depth and extend previous observations on GDPH-defective variants. We found that 36 hours post-transfection, all the N-terminal mutants, like the WT protein, were exposed on the plasma membrane whereas exposure of GDPH-defective variants was significantly reduced. Through electron microscopy and morphometric analyses we demonstrated that the export of G99V is delayed compared to that of WT, with the maximal delay occurring 6-12 hours after transfection, when G99V was found to be highly retained in the endoplasmic reticulum. Binding assays showed that all variants, except C80R, were significantly reduced on the plasma membrane 24-30 hours after transfection. The discrepancy between the time delay observed by morphometric analysis and binding assays might be related to the higher sensitivity of electron microscopy and morphometric analysis as compared to that of binding assay, and to the different transfection conditions, including the amount of DNA used for transfection. Retention of misfolded proteins in the endoplasmic reticulum has been described in several diseases:[18] defective trafficking of mutant uromodulin to the plasma membrane occurs in medullary cystic kidney disease/familial juvenile hyperuricemic nephropathy because of delayed exit of the protein from the endoplasmic reticulum.[13]

Independently of their plasma membrane localization, all the N-terminal mutants studied were unable to activate hepcidin in a promoter luciferase based assay. As shown in Figure 4 their activity was the same as that of a mock construct and plasma membrane-defective mutants such as G320V and D172E.[11] The BMP-SMAD pathway plays an important role in hepcidin regulation. BMP2/4/9 upregulate hepcidin gene transcription and HJV, acting as a BMP-co-receptor, strongly potentiates this signal.[8] The induction of hepcidin by holotransferrin, in primary mouse hepatocyte cell cultures, is mediated by the HJV-BMP2/4-dependent pathway and independent of the HJV-BMP9 pathway.[19] The *in vivo* hepcidin response to an acute administration of iron by injection or ingestion is rapid and proportional to the rise of transferrin saturation.[19]

HJV mutants that do not efficiently reach the plasma membrane cannot interact correctly with BMP/BMP-receptor complexes on the cell surface. However, C80R, G99V and ΔRGD, although exported to the plasma membrane, are excluded from this pathway and are unable to activate the hepcidin response. Although C80R is present on the cell surface, and its export is apparently not delayed, it does not activate hepcidin. This would suggest that delayed export could play a role, but that other molecular mechanisms are crucial to the pathogenesis of the disease. HJV is hypothesized to be present on cell surface in a complex with other proteins such as BMP receptors,[20,21] neogenin[22,23] and perhaps hemochromatosis proteins (HFE, TfR2);[24] one possibility is that C80R, as well as the other N-terminal mutants, interacts abnormally with key surface proteins within the complex.[25]

We confirm distinct trafficking for GDPH-defective mutants. Both D172E and A168D remain uncleaved and are inadequately exposed on plasma membrane. Morphometric analysis showed that D172E, like F170S, although partially retained in the endoplasmic reticulum, is found in the Golgi apparatus.[11] Perhaps these mutants are confined in the Golgi apparatus because of their misfolded conformation, and could then be addressed to a degradation system, as shown for other mutant proteins, such as tissue-non-specific alkaline phosphatase.[26]

After a detailed study of ten HJV pathogenetic mutants and one artificial variant, we clustered them into two broad groups (Table 2): N-terminal variants, which mature properly and are exported to the cell surface, and C-terminal variants, which, unable to undergo autoproteolysis, are retained in the endoplasmic reticulum and have impaired plasma membrane-presentation. s-HJV is produced by all the N-terminal mutants. While the 42 kDa isoform is released into the extracellular environment by a furin pro-convertase that is activated

Table 2. Scheme of maturation and processing of HJV WT and mutants.

		N-terminal variants					*C-terminal (and GDPH-defective) variants*					
	WT	*C80R*	*S85P*	*G99V*	*DRGD*	*C119F*	*A168D*	*F170S*	*D172E*	*W191C*	*G320V*	*R326X*
Endoplasmic reticulum	+	nd	nd	++	nd	nd	nd	++	++	+++	+++	+++
Golgi	+++	nd	nd	++	nd	nd	nd	+++	+++	+	+	+
GDPH cleavage	YES	YES	YES	YES	YES	YES	NO	NO	NO	NO	NO	nd
Plasma membrane (24-30 h)	++	++	+	+	+	+	nd	nd	nd	nd	nd	nd
Plasma membrane (36 h)	+++	+++	+++	+++	+++	++	+	+	+	+	+	-
Medium	+++	+++	+++	+++	+++	+	++	+++	+++	+++	+	+++
Hepcidin activation	YES	NO	nd	NO	NO	nd	nd	nd	NO	nd	NO	nd

nd: not determined.

in hypoxia,[5,6] the origin of the 30 kDa soluble species is still unclear. We have hypothesized that it is shed from m-HJV in hypoxia in order to decrease BMP signaling.[6] The membrane origin of this species is compatible with the observation that only the N-terminal mutants, properly cleaved and exposed to the cell surface, are able to release this isoform.

Based on our present and previous results we suggest that impairment of intracellular trafficking, inadequate plasma membrane presentation or abnormal surface interactions could alter the proper response of most HJV variants to extracellular stimuli. This is reflected by no or very low hepcidin activation, which is the hallmark of juvenile hemochromatosis.

Authorship and Disclosures

AP designed the experimental work, performed the research and co-wrote the manuscript; LS designed the experimental work, performed the research and analyzed the data; AN performed research and analyzed data, CC designed the research and wrote the manuscript. The authors reported no potential conflicts of interest.

References

1. Papanikolaou G, Samuels ME, Ludwig EH, MacDonald ML, Franchini PL, Dube MP, et al. Mutations in HFE2 cause iron overload in chromosome 1q-linked juvenile hemochromatosis. Nat Genet 2004;36:77-82.
2. Roetto A, Papanikolaou G, Politou M, Alberti F, Girelli D, Christakis J, et al. Mutant antimicrobial peptide hepcidin is associated with severe juvenile hemochromatosis. Nat Genet 2003;33:21-2.
3. Huang FW, Pinkus JL, Pinkus GS, Fleming MD, Andrews NC. A mouse model of juvenile hemochromatosis. J Clin Invest 2005;115: 2187-91.
4. Niederkofler V, Salie R, Arber S. Hemojuvelin is essential for dietary iron sensing, and its mutation leads to severe iron overload. J Clin Invest 2005;115:2180-6.
5. Lin L, Nemeth E, Goodnough JB, Thapa DR, Gabayan V, Ganz T. Soluble hemojuvelin is released by proprotein convertase-mediated cleavage at a conserved polybasic RNRR site. Blood Cells Mol Dis 2008;40:122-31.
6. Silvestri L, Pagani A, Camaschella C. Furin-mediated release of soluble hemojuvelin: a new link between hypoxia and iron homeostasis. Blood 2008;111:924-31.
7. Kuninger D, Kuns-Hashimoto R, Kuzmickas R, Rotwein P. Complex biosynthesis of the muscle-enriched iron regulator RGMc. J Cell Sci 2006; 119:3273-83.
8. Babitt JL, Huang FW, Wrighting DM, Xia Y, Sidis Y, Samad TA, et al. Bone morphogenetic protein signaling by hemojuvelin regulates hepcidin expression. Nat Genet 2006; 38:531-9.
9. Wang RH, Li C, Xu X, Zheng Y, Xiao C, Zerfas P, et al. A role of SMAD4 in iron metabolism through the positive regulation of hepcidin expression. Cell Metabol 2005;2:399-409.
10. Lin L, Goldberg YP, Ganz T. Competitive regulation of hepcidin mRNA by soluble and cell-associated hemojuvelin. Blood 2005;106: 2884-9.
11. Silvestri L, Pagani A, Fazi C, Gerardi G, Levi S, Arosio P, et al. Defective targeting of hemojuvelin to plasma membrane is a common pathogenetic mechanism in juvenile hemochromatosis. Blood 2007;109: 4503-10.
12. Lam-Yuk-Tseung S, Camaschella C, Iolascon A, Gros P. A novel R416C mutation in human DMT1 (SLC11A2) displays pleiotropic effects on function and causes microcytic anemia and hepatic iron overload. Blood Cells Mol Dis 2006; 36:347-54.
13. Bernascone I, Vavassori S, Di Pentima A, Santambrogio S, Lamorte G, Amoroso A, et al. Defective intracellular trafficking of uromodulin mutant isoforms. Traffic 2006;7: 1567-79.
14. Polishchuk EV, Di Pentima A, Luini A, Polishchuk RS. Mechanism of constitutive export from the Golgi: bulk flow via the formation, protrusion, and en bloc cleavage of large trans-Golgi network tubular domains. Mol Biol Cell 2003;14:4470-85.
15. Truksa J, Peng H, Lee P, Beutler E. Different regulatory elements are required for response of hepcidin to interleukin-6 and bone morphogenetic proteins 4 and 9. Br J Haematol 2007;139:138-47.
16. Lee PL, Beutler E, Rao SV, Barton JC. Genetic abnormalities and juvenile hemochromatosis: mutations of the HJV gene encoding hemojuvelin. Blood 2004;103:4669-71.
17. Roetto A, Camaschella C. New insights into iron homeostasis through the study of non-HFE hereditary haemochromatosis. Best Pract Res Clin Haematol 2005;18: 235-50.
18. Gregersen N. Protein misfolding disorders: pathogenesis and intervention. J Inherit Metab Dis 2006;29: 456-70.
19. Lin L, Valore EV, Nemeth E, Goodnough JB, Gabayan V, Ganz T. Iron transferrin regulates hepcidin synthesis in primary hepatocyte culture through hemojuvelin and BMP2/4. Blood 2007;110:2182-9.
20. Babitt JL, Huang FW, Xia Y, Sidis Y, Andrews NC, Lin HY. Modulation of bone morphogenetic protein signaling in vivo regulates systemic iron balance. J Clin Invest 2007;117: 1933-9.
21. Xia Y, Babitt JL, Sidis Y, Chung RT, Lin HY. Hemojuvelin regulates hepcidin expression via a selective subset of BMP ligands and receptors independently of neogenin. Blood 2008;111:5195-204.
22. Zhang AS, West AP Jr, Wyman AE, Bjorkman PJ, Enns CA. Interaction of hemojuvelin with neogenin results in iron accumulation in human embryonic kidney 293 cells. J Biol Chem 2005;280:33885-94.
23. Zhang AS, Anderson SA, Meyers KR, Hernandez C, Eisenstein RS, Enns CA. Evidence that inhibition of hemojuvelin shedding in response to iron is mediated through neogenin. J Biol Chem 2007;282: 12547-56.
24. Goswami T, Andrews NC. Hereditary hemochromatosis protein, HFE, interaction with transferrin receptor 2 suggests a molecular mechanism for mammalian iron sensing. J Biol Chem 2006;281: 28494-8.
25. Kuns-Hashimoto R, Kuninger D, Nili M, Rotwein P. Selective binding of RGMc/hemojuvelin, a key protein in systemic iron metabolism, to BMP-2 and neogenin. Am J Physiol Cell Physiol 2008;294:C994-C1003.
26. Brun-Heath I, Lia-Baldini AS, Maillard S, Taillandier A, Utsch B, Nunes ME, et al. Delayed transport of tissue-nonspecific alkaline phosphatase with missense mutations causing hypophosphatasia. Eur J Med Genet 2007;50:367-78.